

Figure 4. Western blot (WB) analysis and corresponding peptographs of (A) STAT1 and (B)  $\delta$ -catenin in ER, LR, AJ, and NL tissues. The tissue used was the sample 18 (NL), 24 (AJ), 37 (LR), and 16 (ER) listed in Supplemental Table 1 in the Supporting Information, respectively. The peptographs are rotated 90° and their widths are reduced (relative Figure 3) to facilitate comparison.

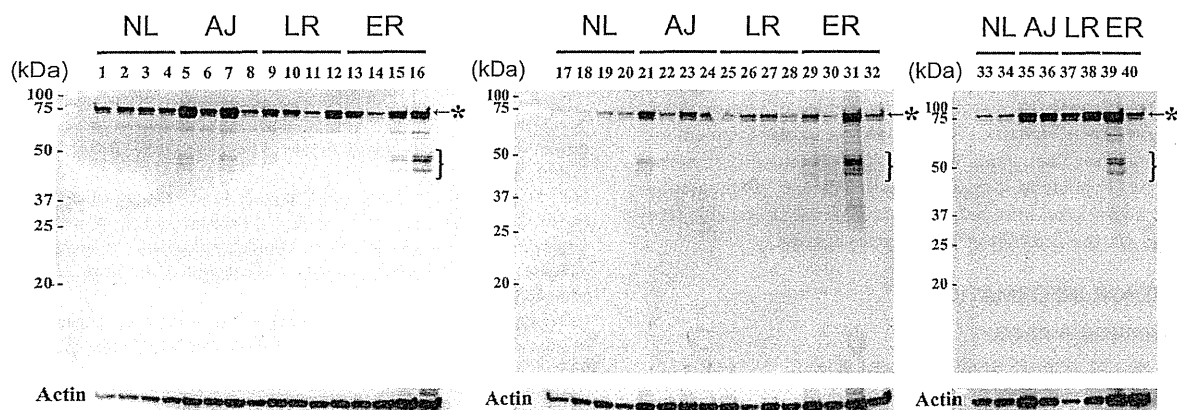


Figure 5. Western blot analysis of STAT1 in clinical tissue samples. The asterisk indicates the expected position of STAT1 according to the calculated molecular weight, and the bracket indicates the expected position of STAT1 peptide fragments according to MS. Note that the STAT1 peptide fragments were observed in a wide range of molecular weight using a gradient SDS-PAGE gel, and the main bands were observed at the expected molecular weight according to the PROTOMAP data. The sample information is given in Supplementary Table 1 in the Supporting Information. Actin was used as a loading control for the evaluation of protein quantities applied to the gel.

in three of these five ER-HCC cases (cases 5, 7 and 21, Figure 5). The STAT1 fragments were not observed in the 10 specimens from patients without recurrence within 2 years after surgery (i.e., patients with LR-HCC). These results suggest that ER-HCC tissues may be heterogeneous in terms of expression and proteolysis of STAT1. This is the first report of a potential functional role of STAT1 proteolysis in the recurrence of cancer, and further investigation of this role will expand our understanding of the biology of HCC. Moreover, these STAT1

proteolysis fragments may serve as a prognostic biomarker and may also lead to novel therapeutic strategies.

## CONCLUSIONS

Here we have presented the first large-scale PROTOMAP profiling of HCC and surrounding liver tissues, which was aimed at the discovery of biomarker candidates for early prediction of the likelihood of recurrence. This analysis identified ~8500 unique proteins and a subset of ~87

biomarker candidates with significantly altered levels in ER-HCC tissues. This protein subset contains many previously identified tumor biomarker candidates (Tables 1 and 2) and proteins with characteristic functional features; specifically, many of the up-regulated proteins are phosphoproteins with roles in signal transduction pathways, and many of the down-regulated proteins are involved in liver function pathways such as the urea cycle and detoxification metabolism. The most notable result of this study may be that proteolytic events appear to occur more frequently during tumorigenesis or recurrence of HCC than during normal liver proliferation. In particular, STAT1, a key transcriptional regulator of the JAK-STAT apoptotic signal transduction pathway, was proteolyzed specifically near the middle of the molecule in ER-HCC tissues, suggesting that the resulting STAT1 fragments may have pathological relevance and diagnostic potential for HCC. Likewise, we note that the aberrant proteolysis of  $\delta$ -catenin may also have a role in HCC recurrence. Determination of the precise immunohistochemical localization of identified proteins using a proteome-wide antibody library such as Human Protein Atlas will be one of the intriguing challenges of our study. Finally, this study suggests that the PROTOMAP strategy will be useful in investigating the pathogenesis of ER-HCC and in identifying key potential biomarkers. The data set presented in this study will also likely serve as a useful resource for future HCC proteomics.

## ■ ASSOCIATED CONTENT

### 📄 Supporting Information

Supplementary Figure 1: The molecular weight (A), subcellular distribution (B), and functional role (C) of proteins identified in this study. Supplementary Table 1: Clinicopathological features of donors. Supplementary Table 2: The peptides identified from ER by the PROTOMAP analysis. Supplementary Table 3: The peptides identified from LR by the PROTOMAP analysis. Supplementary Table 4: The peptides identified from AJ by the PROTOMAP analysis. Supplementary Table 5: The peptides identified from NL by the PROTOMAP analysis. Supplementary Table 6: Peptographs of HCC and related liver tissues. This material is available free of charge via the Internet at <http://pubs.acs.org>.

## ■ AUTHOR INFORMATION

### Corresponding Authors

\*T.I.: Tel: +81 426 77 5667. Fax: +81 426 77 2525. E-mail: [isobe-toshiaki@tmu.ac.jp](mailto:isobe-toshiaki@tmu.ac.jp).

\*T.K.: Tel: +81 3 3542 2511 (ext. 3004). Fax +81 3 3547 5298. E-mail: [takondo@ncc.go.jp](mailto:takondo@ncc.go.jp).

### Present Addresses

<sup>▽</sup>N.M.: Department of Surgery, Kumiai Kosei Hospital, 1-1 Nakagiri-machi, Takayama-shi, Gifu 506-8502, Japan.

<sup>○</sup>H.O.: Department of Pathology, School of Medicine, Keio University, 35 Shinanomachi, Shinjuku-ku, Tokyo 160-0016, Japan.

### Notes

The authors declare no competing financial interest.

## ■ ACKNOWLEDGMENTS

This work was supported by a grant for Advanced Scientific Research from the Tokyo Metropolitan Government.

## ■ ABBREVIATIONS:

ADH4, alcohol dehydrogenase 4; DAVID, Database for Annotation, Visualization and Integrated Discovery; emPAI, exponentially modified protein abundance index; ER, early recurrent; LR, late recurrent; AJ, nontumor tissue adjacent to the tumor; NL, normal liver tissue; HCC, hepatocellular carcinoma; JAK, Janus kinase; LC, liquid chromatography; MS, mass spectrometry; MS/MS, tandem mass spectrometry; PAGE, polyacrylamide gel electrophoresis; PROTOMAP, Protein Topography and Migration Analysis Platform; SDS, sodium dodecyl sulfate; STAT, Signal Transducers and Activators of Transcription family protein

## ■ REFERENCES

- (1) Bosch, F. X.; Ribes, J.; Borrás, J. Epidemiology of primary liver cancer. *Semin. Liver Dis.* 1999, 19 (3), 271–285.
- (2) Bruix, J.; Llovet, J. M. Major achievements in hepatocellular carcinoma. *Lancet* 2009, 373 (9664), 614–616.
- (3) Dudek, K.; Kornasiewicz, O.; Remiszewski, P.; Kobryn, K.; Ziarkiewicz-Wroblewska, B.; Gornicka, B.; Zieniewicz, K.; Krawczyk, M. Impact of tumor characteristic on the outcome of liver transplantation in patients with hepatocellular carcinoma. *Transplant. Proc.* 2009, 41 (8), 3135–3137.
- (4) Lim, K. C.; Chow, P. K.; Allen, J. C.; Chia, G. S.; Lim, M.; Cheow, P. C.; Chung, A. Y.; Ooi, L. L.; Tan, S. B. Microvascular invasion is a better predictor of tumor recurrence and overall survival following surgical resection for hepatocellular carcinoma compared to the Milan criteria. *Ann. Surg.* 2011, 254 (1), 108–113.
- (5) Mazzaferro, V.; Llovet, J. M.; Miceli, R.; Bhoori, S.; Schiavo, M.; Mariani, L.; Camerini, T.; Roayaie, S.; Schwartz, M. E.; Grazi, G. L.; Adam, R.; Neuhaus, P.; Salizzoni, M.; Bruix, J.; Forner, A.; De Carlis, L.; Cillo, U.; Burroughs, A. K.; Troisi, R.; Rossi, M.; Gerunda, G. E.; Lerut, J.; Belghiti, J.; Boin, I.; Gugenheim, J.; Rochling, F.; Van Hoek, B.; Majno, P. Predicting survival after liver transplantation in patients with hepatocellular carcinoma beyond the Milan criteria: a retrospective, exploratory analysis. *Lancet Oncol.* 2009, 10 (1), 35–43.
- (6) Poon, R. T. Differentiating early and late recurrences after resection of HCC in cirrhotic patients: implications on surveillance, prevention, and treatment strategies. *Ann. Surg. Oncol.* 2009, 16 (4), 792–794.
- (7) Roayaie, S.; Blume, I. N.; Thung, S. N.; Guido, M.; Fiel, M. I.; Hiotis, S.; Labow, D. M.; Llovet, J. M.; Schwartz, M. E. A system of classifying microvascular invasion to predict outcome after resection in patients with hepatocellular carcinoma. *Gastroenterology* 2009, 137 (3), 850–855.
- (8) Llovet, J. M.; Bruix, J. Novel advancements in the management of hepatocellular carcinoma in 2008. *J. Hepatol.* 2008, 48 (Suppl 1), S20–S37.
- (9) Iizuka, N.; Oka, M.; Yamada-Okabe, H.; Nishida, M.; Maeda, Y.; Mori, N.; Takao, T.; Tamesa, T.; Tangoku, A.; Tabuchi, H.; Hamada, K.; Nakayama, H.; Ishitsuka, H.; Miyamoto, T.; Hirabayashi, A.; Uchimura, S.; Hamamoto, Y. Oligonucleotide microarray for prediction of early intrahepatic recurrence of hepatocellular carcinoma after curative resection. *Lancet* 2003, 361 (9361), 923–929.
- (10) Ye, Q. H.; Qin, L. X.; Forgues, M.; He, P.; Kim, J. W.; Peng, A. C.; Simon, R.; Li, Y.; Robles, A. L.; Chen, Y.; Ma, Z. C.; Wu, Z. Q.; Ye, S. L.; Liu, Y. K.; Tang, Z. Y.; Wang, X. W. Predicting hepatitis B virus-positive metastatic hepatocellular carcinomas using gene expression profiling and supervised machine learning. *Nat. Med.* 2003, 9 (4), 416–423.
- (11) Du, Y.; Cao, G. W. Challenges of incorporating gene expression data to predict HCC prognosis in the age of systems biology. *World J. Gastroenterol.* 2012, 18 (30), 3941–3944.
- (12) Orimo, T.; Ojima, H.; Hiraoka, N.; Saito, S.; Kosuge, T.; Kakisaka, T.; Yokoo, H.; Nakanishi, K.; Kamiyama, T.; Todo, S.; Hirohashi, S.; Kondo, T. Proteomic profiling reveals the prognostic

value of adenomatous polyposis coli-end-binding protein 1 in hepatocellular carcinoma. *Hepatology* 2008, 48 (6), 1851–1863.

(13) Bai, D. S.; Dai, Z.; Zhou, J.; Liu, Y. K.; Qiu, S. J.; Tan, C. J.; Shi, Y. H.; Huang, C.; Wang, Z.; He, Y. F.; Fan, J. Capn4 overexpression underlies tumor invasion and metastasis after liver transplantation for hepatocellular carcinoma. *Hepatology* 2009, 49 (2), 460–470.

(14) Yi, X.; Luk, J. M.; Lee, N. P.; Peng, J.; Leng, X.; Guan, X. Y.; Lau, G. K.; Beretta, L.; Fan, S. T. Association of mortalin (HSPA9) with liver cancer metastasis and prediction for early tumor recurrence. *Mol. Cell. Proteomics* 2008, 7 (2), 315–325.

(15) Kanamori, H.; Kawakami, T.; Effendi, K.; Yamazaki, K.; Mori, T.; Ebinuma, H.; Masugi, Y.; Du, W.; Nagasaka, K.; Ogiwara, A.; Kyono, Y.; Tanabe, M.; Saito, H.; Hibi, T.; Sakamoto, M. Identification by differential tissue proteome analysis of talin-1 as a novel molecular marker of progression of hepatocellular carcinoma. *Oncology* 2011, 80 (5–6), 406–415.

(16) Lee, S. H.; Shin, M. S.; Lee, H. S.; Bae, J. H.; Lee, H. K.; Kim, H. S.; Kim, S. Y.; Jang, J. J.; Joo, M.; Kang, Y. K.; Park, W. S.; Park, J. Y.; Oh, R. R.; Han, S. Y.; Lee, J. H.; Kim, S. H.; Lee, J. Y.; Yoo, N. J. Expression of Fas and Fas-related molecules in human hepatocellular carcinoma. *Hum. Pathol.* 2001, 32 (3), 250–256.

(17) Volkmann, M.; Schiff, J. H.; Hajjar, Y.; Otto, G.; Stilgenbauer, F.; Fiehn, W.; Galle, P. R.; Hofmann, W. J. Loss of CD95 expression is linked to most but not all p53 mutants in European hepatocellular carcinoma. *J. Mol. Med. (Heidelberg, Ger.)* 2001, 79 (10), 594–600.

(18) Marquardt, J. U.; Galle, P. R.; Teufel, A. Molecular diagnosis and therapy of hepatocellular carcinoma (HCC): an emerging field for advanced technologies. *J. Hepatol.* 2012, 56 (1), 267–275.

(19) Turgeon, V. L.; Houenou, L. J. The role of thrombin-like (serine) proteases in the development, plasticity and pathology of the nervous system. *Brain Res. Rev.* 1997, 25 (1), 85–95.

(20) Riewald, M.; Ruf, W. Mechanistic coupling of protease signaling and initiation of coagulation by tissue factor. *Proc. Natl. Acad. Sci. U. S. A.* 2001, 98 (14), 7742–7747.

(21) Alnemri, E. S. Mammalian cell death proteases: a family of highly conserved aspartate specific cysteine proteases. *J. Cell Biochem.* 1997, 64 (1), 33–42.

(22) Abdel-Rahman, H. M.; Kimura, T.; Hidaka, K.; Kiso, A.; Nezami, A.; Freire, E.; Hayashi, Y.; Kiso, Y. Design of inhibitors against HIV, HTLV-I, and Plasmodium falciparum aspartic proteases. *Biol. Chem.* 2004, 385 (11), 1035–1039.

(23) van Kempen, L. C.; de Visser, K. E.; Coussens, L. M. Inflammation, proteases and cancer. *Eur. J. Cancer* 2006, 42 (6), 728–734.

(24) Quesada, V.; Ordóñez, G. R.; Sanchez, L. M.; Puente, X. S.; Lopez-Otin, C. The Degradome database: mammalian proteases and diseases of proteolysis. *Nucleic Acids Res.* 2009, 37 (Database issue), D239–D243.

(25) Nisman, B.; Biran, H.; Heching, N.; Barak, V.; Ramu, N.; Nemirovsky, I.; Peretz, T. Prognostic role of serum cytokeratin 19 fragments in advanced non-small-cell lung cancer: association of marker changes after two chemotherapy cycles with different measures of clinical response and survival. *Br. J. Cancer* 2008, 98 (1), 77–79.

(26) Streckfus, C.; Bigler, L.; Tucci, M.; Thigpen, J. T. A preliminary study of CA15–3, c-erbB-2, epidermal growth factor receptor, cathepsin-D, and p53 in saliva among women with breast carcinoma. *Cancer Invest.* 2000, 18 (2), 101–109.

(27) Dix, M. M.; Simon, G. M.; Cravatt, B. F. Global mapping of the topography and magnitude of proteolytic events in apoptosis. *Cell* 2008, 134 (4), 679–691.

(28) Shen, C.; Yu, Y.; Li, H.; Yan, G.; Liu, M.; Shen, H.; Yang, P. Global profiling of proteolytically modified proteins in human metastatic hepatocellular carcinoma cell lines reveals CAPN2 centered network. *Proteomics* 2012, 12 (12), 1917–1927.

(29) Ishihama, Y.; Oda, Y.; Tabata, T.; Sato, T.; Nagasu, T.; Rappsilber, J.; Mann, M. Exponentially modified protein abundance index (emPAI) for estimation of absolute protein amount in proteomics by the number of sequenced peptides per protein. *Mol. Cell. Proteomics* 2005, 4 (9), 1265–1272.

(30) Taoka, M.; Wakamiya, A.; Nakayama, H.; Isobe, T. Protein profiling of rat cerebella during development. *Electrophoresis* 2000, 21 (9), 1872–1879.

(31) Abiko, M.; Furuta, K.; Yamauchi, Y.; Fujita, C.; Taoka, M.; Isobe, T.; Okamoto, T. Identification of proteins enriched in rice egg or sperm cells by single-cell proteomics. *PLoS One* 2013, 8 (7), e69578.

(32) Taoka, M.; Yamauchi, Y.; Nobe, Y.; Masaki, S.; Nakayama, H.; Ishikawa, H.; Takahashi, N.; Isobe, T. An analytical platform for mass spectrometry-based identification and chemical analysis of RNA in ribonucleoprotein complexes. *Nucleic Acids Res.* 2009, 37 (21), e140.

(33) Shinkawa, T.; Taoka, M.; Yamauchi, Y.; Ichimura, T.; Kaji, H.; Takahashi, N.; Isobe, T. STEM: a software tool for large-scale proteomic data analyses. *J. Proteome Res.* 2005, 4 (5), 1826–1831.

(34) Corrocher, R.; Casaril, M.; Bellisola, G.; Gabrielli, G. B.; Nicoli, N.; Guidi, G. C.; De Sandre, G. Severe impairment of antioxidant system in human hepatoma. *Cancer* 1986, 58 (8), 1658–1662.

(35) Sato, K.; Ito, K.; Kohara, H.; Yamaguchi, Y.; Adachi, K.; Endo, H. Negative regulation of catalase gene expression in hepatoma cells. *Mol. Cell. Biol.* 1992, 12 (6), 2525–2533.

(36) Sun, Y.; Oberley, L. W.; Oberley, T. D.; Elwell, J. H.; Sierra-Rivera, E. Lowered antioxidant enzymes in spontaneously transformed embryonic mouse liver cells in culture. *Carcinogenesis* 1993, 14 (7), 1457–1463.

(37) Qiu, W.; David, D.; Zhou, B.; Chu, P. G.; Zhang, B.; Wu, M.; Xiao, J.; Han, T.; Zhu, Z.; Wang, T.; Liu, X.; Lopez, R.; Frankel, P.; Jong, A.; Yen, Y. Down-regulation of growth arrest DNA damage-inducible gene 45beta expression is associated with human hepatocellular carcinoma. *Am. J. Pathol.* 2003, 162 (6), 1961–1974.

(38) Ho, J. C.; Cheung, S. T.; Leung, K. L.; Ng, I. O.; Fan, S. T. Decreased expression of cytochrome P450 2E1 is associated with poor prognosis of hepatocellular carcinoma. *Int. J. Cancer* 2004, 111 (4), 494–500.

(39) Ngoka, L. C. Dramatic down-regulation of oxidoreductases in human hepatocellular carcinoma hepG2 cells: proteomics and gene ontology unveiling new frontiers in cancer enzymology. *Proteome Sci.* 2008, 6, 29.

(40) Wei, R. R.; Zhang, M. Y.; Rao, H. L.; Pu, H. Y.; Zhang, H. Z.; Wang, H. Y. Identification of ADH4 as a novel and potential prognostic marker in hepatocellular carcinoma. *Med. Oncol* 2012, 29 (4), 2737–2743.

(41) Jordan, C. T.; Guzman, M. L.; Noble, M. Cancer stem cells. *N. Engl. J. Med.* 2006, 355 (12), 1253–1261.

(42) Stark, G. R.; Darnell, J. E., Jr. The JAK-STAT pathway at twenty. *Immunity* 2012, 36 (4), 503–514.

(43) Chen, X.; Vinkemeier, U.; Zhao, Y.; Jeruzalmi, D.; Darnell, J. E., Jr.; Kuriyan, J. Crystal structure of a tyrosine phosphorylated STAT-1 dimer bound to DNA. *Cell* 1998, 93 (5), 827–839.

(44) Menke, A.; Giehl, K. Regulation of adherens junctions by Rho GTPases and p120-catenin. *Arch. Biochem. Biophys.* 2012, 524 (1), 48–55.

(45) McCrea, P. D.; Park, J. I. Developmental functions of the P120-catenin sub-family. *Biochim. Biophys. Acta* 2007, 1773 (1), 17–33.

(46) Ishiyama, N.; Lee, S. H.; Liu, S.; Li, G. Y.; Smith, M. J.; Reichardt, L. F.; Ikura, M. Dynamic and static interactions between p120 catenin and E-cadherin regulate the stability of cell-cell adhesion. *Cell* 2010, 141 (1), 117–128.

(47) Torbenson, M.; Wang, J.; Choti, M.; Ashfaq, R.; Maitra, A.; Wilentz, R. E.; Boitnott, J. Hepatocellular carcinomas show abnormal expression of fibronectin protein. *Mod. Pathol.* 2002, 15 (8), 826–830.

(48) Matsui, S.; Takahashi, T.; Oyanagi, Y.; Takahashi, S.; Boku, S.; Takahashi, K.; Furukawa, K.; Arai, F.; Asakura, H. Expression, localization and alternative splicing pattern of fibronectin messenger RNA in fibrotic human liver and hepatocellular carcinoma. *J. Hepatol.* 1997, 27 (5), 843–853.

(49) Haglund, C.; Ylatupa, S.; Mertaniemi, P.; Partanen, P. Cellular fibronectin concentration in the plasma of patients with malignant and benign diseases: a comparison with CA 19–9 and CEA. *Br. J. Cancer* 1997, 76 (6), 777–783.

(50) Chen, X. L.; Zhou, L.; Yang, J.; Shen, F. K.; Zhao, S. P.; Wang, Y. L. Hepatocellular carcinoma-associated protein markers investigated by MALDI-TOF MS. *Mol. Med. Rep.* 2011, 3 (4), 589–596.

(51) Luk, J. M.; Lam, C. T.; Situ, A. F.; Lam, B. Y.; Ng, I. O.; Hu, M. Y.; Che, C. M.; Fan, S. T. Proteomic profiling of hepatocellular carcinoma in Chinese cohort reveals heat-shock proteins (Hsp27, Hsp70, GRP78) up-regulation and their associated prognostic values. *Proteomics* 2006, 6 (3), 1049–1057.

(52) Song, H. Y.; Liu, Y. K.; Feng, J. T.; Cui, J. F.; Dai, Z.; Zhang, L. J.; Feng, J. X.; Shen, H. L.; Tang, Z. Y. Proteomic analysis on metastasis-associated proteins of human hepatocellular carcinoma tissues. *J. Cancer Res. Clin. Oncol.* 2006, 132 (2), 92–98.

(53) Yokota, S.; Yamamoto, Y.; Shimizu, K.; Momoji, H.; Kamikawa, T.; Yamaoka, Y.; Yanagi, H.; Yura, T.; Kubota, H. Increased expression of cytosolic chaperonin CCT in human hepatocellular and colonic carcinoma. *Cell Stress Chaperones* 2001, 6 (4), 345–350.

(54) Sung, Y. K.; Hwang, S. Y.; Park, M. K.; Bae, H. I.; Kim, W. H.; Kim, J. C.; Kim, M. Fatty acid-CoA ligase 4 is overexpressed in human hepatocellular carcinoma. *Cancer Sci.* 2003, 94 (5), 421–424.

(55) Liu, H.; Dong, H.; Robertson, K.; Liu, C. DNA methylation suppresses expression of the urea cycle enzyme carbamoyl phosphate synthetase 1 (CPS1) in human hepatocellular carcinoma. *Am. J. Pathol.* 2011, 178 (2), 652–661.

(56) Cardona, D. M.; Zhang, X.; Liu, C. Loss of carbamoyl phosphate synthetase I in small-intestinal adenocarcinoma. *Am. J. Clin. Pathol.* 2009, 132 (6), 877–882.

(57) Butler, S. L.; Dong, H.; Cardona, D.; Jia, M.; Zheng, R.; Zhu, H.; Crawford, J. M.; Liu, C. The antigen for Hep Par 1 antibody is the urea cycle enzyme carbamoyl phosphate synthetase 1. *Lab. Invest.* 2008, 88 (1), 78–88.

(58) Matos, J. M.; Witzmann, F. A.; Cummings, O. W.; Schmidt, C. M. A pilot study of proteomic profiles of human hepatocellular carcinoma in the United States. *J. Surg. Res.* 2009, 155 (2), 237–243.

(59) Sigrüener, A.; Buechler, C.; Orso, E.; Hartmann, A.; Wild, P. J.; Terracciano, L.; Roncalli, M.; Bornstein, S. R.; Schmitz, G. Human aldehyde oxidase 1 interacts with ATP-binding cassette transporter-1 and modulates its activity in hepatocytes. *Horm. Metab. Res.* 2007, 39 (11), 781–789.

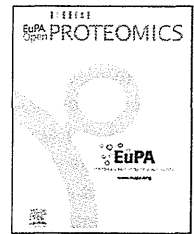
(60) Chen, M.; Zhang, J.; Li, N.; Qian, Z.; Zhu, M.; Li, Q.; Zheng, J.; Wang, X.; Shi, G. Promoter hypermethylation mediated down-regulation of FBPI in human hepatocellular carcinoma and colon cancer. *PLoS One* 2011, 6 (10), e25564.

(61) Liu, Z.; Ma, Y.; Yang, J.; Qin, H. Upregulated and downregulated proteins in hepatocellular carcinoma: a systematic review of proteomic profiling studies. *OMICS* 2011, 15 (1–2), 61–71.

(62) Chen, X. Q.; He, J. R.; Wang, H. Y. Decreased expression of ALDH1L1 is associated with a poor prognosis in hepatocellular carcinoma. *Med. Oncol.* 2012, 29 (3), 1843–1849.

Available online at [www.sciencedirect.com](http://www.sciencedirect.com)

ScienceDirect

journal homepage: <http://www.elsevier.com/locate/euprot>

# Approach to spot overlapping problem in 2D-PAGE revealed clinical and functional significance of RKIP and MnSOD in renal cell carcinoma

Noriyuki Hosoya<sup>a,b</sup>, Marimu Sakumoto<sup>a</sup>, Yoshihiko Tomita<sup>b</sup>,  
Tadashi Kondo<sup>a,\*</sup>

<sup>a</sup> Division of Pharmacoproteomics, National Cancer Center Research Institute, Tokyo, Japan

<sup>b</sup> Department of Urology, Yamagata University Faculty of Medicine, Yamagata, Japan

## ARTICLE INFO

### Article history:

Received 14 November 2013

Received in revised form

18 June 2014

Accepted 26 June 2014

Available online 5 July 2014

### Keywords:

Spot overlapping

2D-PAGE

Mass spectrometry

Renal cell carcinoma

raf-1 kinase inhibitory protein

Manganese superoxide dismutase

## ABSTRACT

Previously, we identified protein spots with differential intensity between normal and tumor tissues of renal cell carcinoma (RCC) using 2D-DIGE. Here, we further examined two proteins, raf-1 kinase inhibitory protein (RKIP) and manganese superoxide dismutase (MnSOD), identified in one protein spot. Western blotting demonstrated that RKIP and MnSOD exhibited opposite expression patterns in normal and tumor tissues. Immunohistochemistry showed that MnSOD level significantly correlated with shorter progression-free survival. Gene-silencing assay demonstrated that RKIP and MnSOD had suppressive and promotive effects on tumor cell proliferation and invasion, respectively. Our findings reveal biological and clinical significance of RKIP and MnSOD in RCC.

© 2014 The Authors. Published by Elsevier B.V. on behalf of European Proteomics Association (EuPA). This is an open access article under the CC BY-NC-ND license (<http://creativecommons.org/licenses/by-nc-nd/3.0/>).

## 1. Introduction

Two-dimensional polyacrylamide gel electrophoresis (2D-PAGE) is one of the most popular methods widely used in medical proteomic studies [1]. This method demonstrates the highest protein separation performance, after mass spectrometry (MS), by separating proteins according to two independent physical parameters such as isoelectric point and molecular weight. In the last three decades, the separation performance of 2D-PAGE has been improved by incorporating novel technologies. Firstly, reproducibility of protein profiling

was dramatically improved by the introduction of immobilized pH gradient gels to isoelectric focusing separation [2]. Secondly, advances in modern technologies such as MS and database search enabled identification of the proteins included in protein spots [3]. Thirdly, novel fluorescent protein labeling dyes made it possible to simultaneously analyze multiple protein samples in a single gel, thus compensating for gel-to-gel variations (two-dimensional difference gel electrophoresis, 2D-DIGE) [4]. With these three innovations, 2D-PAGE has emerged as one of the most powerful proteomic tools for protein expression profiling in a variety of research projects.

\* Corresponding author at: Division of Pharmacoproteomics, National Cancer Center Research Institute, 5-1-1 Tsukiji, Chuo-ku, Tokyo 104-0045, Japan. Tel.: +81 3 3542 2511x3004; fax: +81 3 3547 5298.

E-mail address: [takondo@ncc.go.jp](mailto:takondo@ncc.go.jp) (T. Kondo).

<http://dx.doi.org/10.1016/j.euprot.2014.06.005>

2212-9685/© 2014 The Authors. Published by Elsevier B.V. on behalf of European Proteomics Association (EuPA). This is an open access article under the CC BY-NC-ND license (<http://creativecommons.org/licenses/by-nc-nd/3.0/>).

As is the case for all proteomic methods, 2D-PAGE has its inherent limitations, such as spot overlapping. As the expected number of protein spots can reach several thousand, and the separation area of a 2D gel is limited, single protein spots may include multiple protein species. This problem has been frequently encountered, especially when protein identification is performed using a highly sensitive LC-MS/MS technique [5]. Campostrini et al. [6] suggested to resolve this problem by improving separation performance. However, Okano et al. [7] reported that the spot overlapping problem could not be solved even with extensive fractionation of protein samples by multi-dimensional liquid chromatography. Kosaihira et al. used MS to identify multiple proteins from 2D-DIGE protein spots, and demonstrated that the use of large format gels did not solve the spot overlapping problem either. They used large format (24 cm × 33 cm) 2D gels and reported that, of 791 protein spots identified by LC-MS/MS, 391 spots contained multiple proteins, accounting for 45.8% of all protein spots obtained in their studies [8]. Obviously, spot overlapping cannot be resolved by improving the separation performance of 2D-PAGE.

Spot overlapping is a serious problem in a comparative study. When multiple proteins are identified in a single protein spot, it is difficult to determine the contribution of an individual protein to the difference in spot intensity between the compared samples. A protein with the highest identification score and number of peptides for protein identification is usually considered to be the one mostly contributing to the difference in spot intensity, and the other proteins in the spot are not further examined. However, the protein with the highest identification score may not necessarily be the cause of the differential spot intensity; therefore the other proteins in the spot may equally be worth examining. Yet, as a rule, only one protein per spot is investigated in terms of functional and clinical significance.

In our previous study, we performed proteomic comparisons between the tumor and non-tumor tissues of patients with clear cell renal cell carcinoma (ccRCC), which is the most frequent type of renal cell carcinoma (RCC) [9]. RCC is the third most common urological malignancy after prostate and bladder cancers, and further understanding of its molecular background is required to improve the clinical outcome [10]. In the previous study, we examined the ccRCC proteome using 2D-DIGE and identified proteins with aberrant expression in tumor tissues, reporting a novel ccRCC prognostic factor, N-myc downstream-regulated gene 1 (NDRG1). By MS protein identification of 56 protein spots, we found that 37 of them contained multiple proteins. In this study, we focused on one spot, which included raf-1 kinase inhibitory protein (RKIP) and manganese superoxide dismutase (MnSOD). Although these two proteins have been associated with cancer malignancies, their clinical and biological significance for ccRCC has not been established. We found that RKIP and MnSOD had opposite expression patterns in the normal and tumor tissues of ccRCC patients, and although the Mascot score and number of peptides for MnSOD were lower than for RKIP, the intensity of the spot was determined by the MnSOD expression level. Immunohistochemical analysis of patients' tissues and *in vitro* RNA interference experiments revealed the clinical and functional significance of RKIP and MnSOD in ccRCC. Our results

suggest that more than one protein in a single 2D-PAGE protein spot should be considered for further analysis.

## 2. Materials and methods

### 2.1. Patients

This study included 108 patients with ccRCC who underwent curative resection surgery at Yamagata University Hospital from January 2003 to June 2012. All patients in this study had no history of systemic therapies prior to surgery. Tumors were stage-classified according to the Union for International Cancer Control (UICC), 7th TNM Classification of Malignant Tumors [11]. Tumor grades were determined according to the Fuhrman Nuclear Grade [12]. The patients at stage I were selected randomly and all patients at stage II, III, or IV were included in the study. Frozen tissue samples of primary tumors were available from 9 patients and were used for proteomic analysis in our previous study. Formalin-fixed paraffin-embedded (FFPE) tissues from the other 99 patients were used for immunohistochemistry (Table 1, Supplementary Table 1). Patients who offered FFPE tissues were between 35 and 85 years old (median 63 years), and patients' follow-up was conducted between 1 and 119 months (median 24 months). None of the patients received pre-operative cancer treatments. This study was approved by the ethical committee of Yamagata University Faculty of Medicine and National Cancer Center, and informed consent was obtained from all patients in this study.

Supplementary Table 1 related to this article can be found, in the online version, at doi:10.1016/j.euprot.2014.06.005.

### 2.2. Two-dimensional difference gel electrophoresis and mass spectrometric protein identification

Protein expression profiling by 2D-DIGE and protein identification by MS have been performed in our previous study [9], and part of the published proteomic data have been used in this study. The proteomic data were obtained in our previous study as follows [9]. In brief, the tissue samples were extracted using the urea lysis buffer (2 M thiourea, 7 M urea, 3% CHAPS, and 1% Triton X-100). 2D-DIGE was performed by labeling the protein samples with CyDye DIGE Fluor saturation dye (GE, Uppsala, Sweden). The individual samples were labeled with Cy5, and the internal standard sample, which contained a mixture of equal amounts from all individual samples, was labeled with Cy3. These differently labeled samples were mixed and separated by 2D-PAGE. In 2D-PAGE, the first dimension of separation was achieved by IPG gel (24 cm length, pI range between 3 and 10, GE) with Multiphor II (GE), and the second dimension of separation was performed by SDS-PAGE with our original large format electrophoresis apparatus [13]. The gels were scanned by a laser scanner (Typhoon Trio, GE), and gel-to-gel variations were compensated by normalizing the intensities in Cy5 images to those in Cy3 images using image analysis software (Progenesis SameSpot, Non-linear Dynamics, New Castle, UK). Protein identification was achieved using a preparative gel where 100 μg of protein sample was labeled with Cy3. The protein spot was recovered

**Table 1 – Clinicopathological features of the patients and correlation with RKIP and MnSOD expression.**

Features	Overall (n = 99)	RKIP expression			MnSOD expression		
		Low	High	p value	Low	High	p value
All	99	87	12		38	61	
Age							
≤63	50	47	3	0.115 <sup>d</sup>	20	30	0.738 <sup>e</sup>
>63	49	40	9		18	31	
Gender							
Male	71	65	6	0.150 <sup>d</sup>	29	42	0.567 <sup>d</sup>
Female	28	22	6		9	19	
T stage <sup>a</sup>							
1	56	53	3	0.166 <sup>d</sup>	22	34	0.760 <sup>d</sup>
2	12	9	3		6	6	
3	31	25	6		10	21	
Lymph node <sup>a</sup>							
No	94	82	12	0.881 <sup>d</sup>	36	58	0.692 <sup>d</sup>
Yes	5	5	0		2	3	
Metastasis <sup>a</sup>							
No	86	75	11	0.945 <sup>d</sup>	34	52	0.764 <sup>d</sup>
Yes	13	12	1		4	9	
UICC stage <sup>a</sup>							
I	53	50	3	0.213 <sup>d</sup>	21	32	0.951 <sup>d</sup>
II	8	6	2		4	4	
III	24	18	6		9	15	
IV	14	13	1		4	10	
Grade <sup>b</sup>							
1	38	35	3	0.132 <sup>d</sup>	14	24	0.923 <sup>d</sup>
2	37	34	3		16	21	
3	19	13	6		6	13	
4	5	5	0		2	3	
Mode of infiltration <sup>c</sup>							
a	71	65	6	0.150 <sup>d</sup>	29	42	0.567 <sup>d</sup>
b, c	28	22	6		9	19	
Vascular invasion							
No	74	68	6	0.080 <sup>d</sup>	30	44	0.602 <sup>d</sup>
Yes	25	19	6		8	17	

<sup>a</sup> Tumors were staged on the basis of the Union for International Cancer Control seventh edition TNM pathologic classification.

<sup>b</sup> The Fuhrman nuclear grade.

<sup>c</sup> Mode of infiltration was described as follows: expensive (a), tentacular (b) or diffuse (c).

<sup>d</sup> The p value was calculated by Yates Chi-square test.

<sup>e</sup> The p value was calculated by Chi-square test.

by an automated spot recovering machine (Molecular Hunter, AsOne, Osaka, Japan), and proteins were extracted by in-gel tryptic digestion. The peptides were subjected to MS identification (LTQ Orbital XL, ThermoElectron, San Jose, CA). The detailed protocols and proteome data were described in our previous study [9].

### 2.3. SDS-PAGE and Western blotting

Five microgram of protein samples were separated by SDS-PAGE and transferred to PVDF membranes. Membranes were blocked in TBS-T buffer containing 5% skimmed milk for 60 min and incubated with a primary antibody at 4°C overnight and then with a secondary antibody at room temperature for 90 min. The primary and secondary antibodies were used at the following dilutions: RKIP (1:1200; Abcam, Cambridge, UK), MnSOD (1:1000; EPITOMICS, Burlingame, CA), anti-goat IgG (1:4000; Santa Cruz Biotechnology, Santa Cruz, CA), and anti-rabbit IgG (1:2000, GE Healthcare, Uppsala, Sweden). Immunoreactive bands were detected by enhanced chemiluminescence (ECL PRIME, GE) and LAS-3000 (FujiFilm,

Tokyo, Japan). The membranes were stained with Ponceau S to normalize for protein loading [14], and the intensity of the protein bands was measured using imaging software (Image-Quant software, GE). The intensity of an individual protein band was normalized to Ponceau S staining.

### 2.4. Immunohistochemistry

Immunostaining was performed using FFPE tissues. Tissue sections (4 μm thick) were deparaffinized in xylene and rehydrated in decreasing concentrations of ethanol (100% to water), and antigen unmasking was performed by autoclaving in 10 mM citrate buffer at 121°C for 10 min. For RKIP immunostaining, endogenous peroxidase activity was quenched with 3% hydrogen peroxide (Dako, Glostrup, Denmark) for 5 min. Endogenous biotin was blocked using the Biotin-Blocking System (Dako). Tissue sections were blocked with 10% horse serum for 5 min and reacted with anti-RKIP antibody (1:3000) at 4°C overnight. They were further incubated with the secondary antibody for 30 min, and then with streptavidin-peroxidase (Dako) for 30 min at room



temperature; immunoreactivity was detected by incubation with diaminobenzidine (DAB, Dako) for 2 min. Slides were counterstained with hematoxylin. For MnSOD immunostaining, tissue sections were autoclaved in 10 mM citrate buffer, incubated in 0.3% hydrogen peroxide/methanol for 30 min to quench endogenous peroxidase activity, and blocked with 10% horse serum for 5 min. Slides were incubated with anti-MnSOD antibody (1:1000) overnight at 4°C and then with the secondary antibody (EnVision, Dako) for 30 min at room temperature. Immunostaining was visualized by incubation with DAB for 1 min; slides were counterstained with hematoxylin.

Non-tumor renal cortical tissues were used as control. The intensity of RKIP or MnSOD immunostaining was scored according to staining intensity relative to normal proximal tubule cells. The RKIP expression levels in individual cases were classified into low (lower staining intensity than in proximal tubule cells) or high (similar or higher staining intensity than in proximal tubule cells). The MnSOD expression levels were classified into low (similar or lower staining intensity than in proximal tubule cells) or high (higher intensity than in proximal tubule cells).

### 2.5. Cell culture and small interfering RNA

The RCC cell line Caki-1 (TKG0436, the Cell Resource Center for Biomedical Research Institute of Development, Aging and Cancer Tohoku University, Miyagi, Japan) was maintained in RPMI-1640 medium (Wako, Osaka, Japan) containing 10% fetal bovine serum (FBS; Medical & Biological Laboratories, Aichi, Japan), and incubated at 37°C in 5% CO<sub>2</sub>.

Small interfering RNAs (siRNAs) were purchased from Sigma-Aldrich (St. Louis, MO). The sequences of sense and antisense oligonucleotides are shown in Supplementary Table 2. The specific siRNAs or negative control siRNA (Low GC Duplex, Invitrogen, Calsbad, CA) were transfected into the RCC cells using Lipofectamine 2000 transfection reagent (Invitrogen) according to the manufacturer's protocol.

Supplementary Table 2 related to this article can be found, in the online version, at doi:10.1016/j.euprot.2014.06.005.

### 2.6. Cell proliferation assay

The cells were seeded in 96-well plates at 3000 cells/well and transfected with siRNAs targeting RKIP or MnSOD, or control siRNA. Cell viability was measured using Cell Counting Kit-8 (Dojindo, Kumamoto, Japan) and a photometer (SAFIRE, TECAN, Mannedorf, Switzerland) according to the manufacturer's instructions.

### 2.7. Cell invasion assay

*In vitro* tumor cell invasion or migration was measured using the BD Biocoat 8 μm pore-Matrigel Invasion Chambers (BD Biosciences, Bedford, MA). In brief, RCC cells were transfected with RKIP, MnSOD, or control siRNAs. After 24 h, the cells were transferred into serum-free RPMI and plated in the upper chambers at  $2 \times 10^5$  cells/chamber; the bottom chamber contained RPMI with 10% FBS. After incubation for 24 h the cells that migrated across the membrane to the bottom chamber were fixed, stained, and counted in 3 separate fields using

200× magnification. Cell invasion was calculated as the percentage of cells in the matrigel chamber compared to the control chamber (% invasion), and invasion index was calculated by comparing the % invasion with that of the control siRNA-transfected cells. Each experiment was repeated three times.

### 2.8. Statistical analysis

The Chi-square test or Yates Chi-square test was used to assess the relationship between clinico-pathological manifestations and protein expression [15,16]. Kaplan–Meier curves were calculated [17], and the differences between stratified survival functions were assessed using the log-rank test [18]. The independence of each prognostic factor was evaluated using the Cox proportional hazard model [19]. Continuous variables presented as the mean ± standard deviation (SD) fit the criteria for parametricity, and the Student's t-test was used for analysis [20]. The Chi-square test, Yates Chi-square test, and Student's t-test were performed using Microsoft Excel (Microsoft, Redmond, WA). Other data analyses were conducted using StatView 5.0 (SAS Institute, Cary, NC).

## 3. Results and discussion

### 3.1. Different intensity of protein spots between normal and tumor tissues

In this study, we focused on one protein spot, 14991, which contained RKIP and MnSOD. Fig. 1A shows the 2D image with the position of spot 14991. The spot intensity was significantly increased (more than 2-fold; p value less than 0.05) in tumor tissues of 9 ccRCC patients when compared with adjacent normal tissues (Fig. 1A and B). MS protein identification revealed that spot 14991 included RKIP and MnSOD; the Mascot scores of RKIP and MnSOD were 204 and 100, and the numbers of peptides for protein identification were 4 and 2, respectively (Supplementary Table 3). These data have been published in our previous report [9].

Supplementary Table 3 related to this article can be found, in the online version, at doi:10.1016/j.euprot.2014.06.005.

Raf kinase inhibitors such as sorafenib were introduced into the treatments of the RCC patients [21]. RKIP is an endogenous inhibitor of the Ras-Raf-1-MEK1/2-ERK1/2 pathway [22], and decreased RKIP expression was associated with tumor progression and metastasis in a variety of cancers, suggesting tumor suppressive activity of RKIP [23–30]. Recently, Moon et al. [31] reported the association of reduced RKIP expression with malignant transformations in ccRCC. However, the functional effects of reduced RKIP expression in ccRCC tumors have not been examined. Considering that reduced RKIP expression was associated with tumor progression and metastasis in many types of cancers [23–30], the clinical and functional significance of RKIP in ccRCC should be investigated.

MnSOD is a mitochondrial matrix enzyme that converts superoxide to a less reactive hydrogen peroxide, protecting mitochondria against the damaging effects of oxidative stress [32]. The expression patterns and biological role of MnSOD in tumor cells depend on cancer type. Exogenous expression

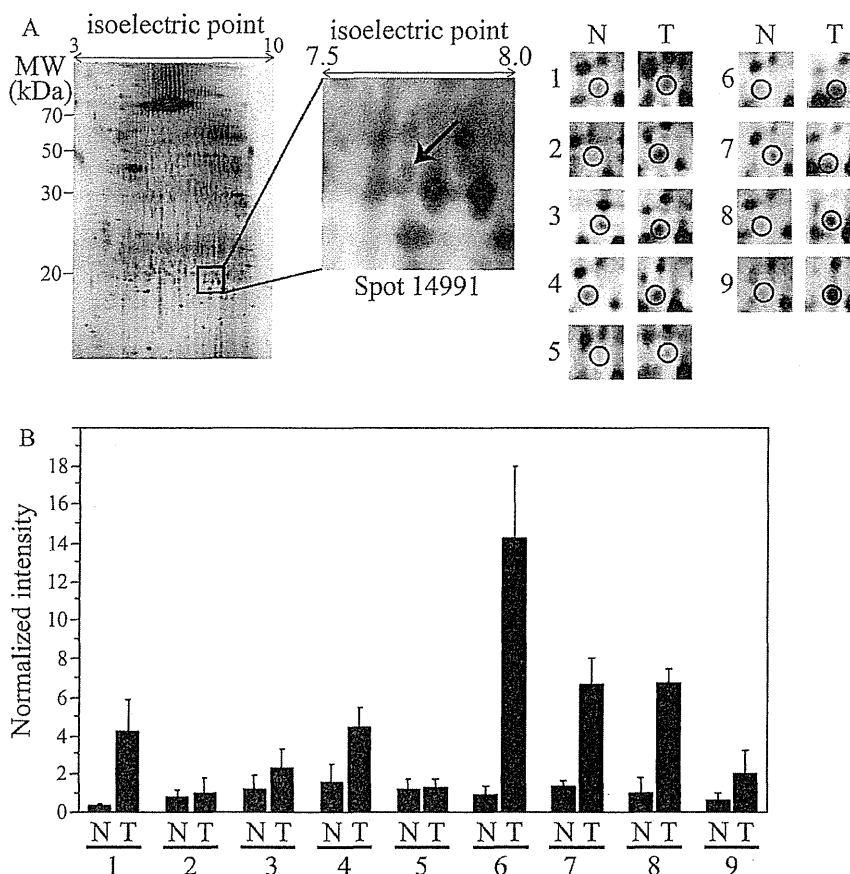


**Fig. 1 – The intensity of spot 14991 was higher in tumor tissues than in non-tumor tissues in clear cell renal cell carcinoma (ccRCC) patients. (A) The position of spot 14991 on 2D-DIGE gel in the 9 ccRCC cases. (B) The normalized spot 14991 intensity. Note that the intensity increased in tumor samples compared to normal tissues.**

of MnSOD inhibited tumor growth in the experimental model of colorectal cancer, suggesting a tumor suppressive role for MnSOD [33,34]. In contrast, MnSOD up-regulation contributed to the progression of cancer metastasis by mechanisms involving inhibition of apoptosis and activation of metalloproteinase-2 [35,36]. There were few papers about the clinical and biological significance of MnSOD in ccRCC. Durak et al. reported up-regulation of MnSOD expression in RCC, but its clinical significance was not examined [37]. As MnSOD plays a fundamental role in physiological and disease conditions [38], and the regulatory mechanisms of oxidative stress are targeted by cancer treatments [39], the biological and clinical role of MnSOD in ccRCC should be investigated.

In this study we investigated the biological and clinical significance of the aberrant regulation of RKIP and MnSOD in ccRCC.

### 3.2. Validation by Western blotting

To validate the expression levels of RKIP and MnSOD in tissue samples, we performed Western blotting. We first examined RKIP expression, as its MasCot score and the number of identified peptides were higher than those of MnSOD (Supplemental Table 3). However, unexpectedly, we found that RKIP expression decreased in tumors compared to normal tissues

(Fig. 2A). On the contrary, when we analyzed MnSOD expression, it appeared to be higher in tumors than in normal tissues (Fig. 2A). The results of quantitative comparison are summarized in Fig. 2B. We therefore concluded that it was MnSOD expression that mostly contributed to the higher intensity of spot 14991.

We further confirmed the differential expression of RKIP and MnSOD in tumor and non-tumor tissues of ccRCC patients by immunohistochemistry. As we extracted proteins by tissue homogenization, differential protein expression could reflect both the proportion of cell populations in a tissue sample and the differential protein expression in a specific cell population. We aimed to distinguish between these two possibilities using immunohistochemistry. We found that RKIP was highly expressed in normal proximal renal tubule cells, and MnSOD was dominantly expressed in tumor cells, suggesting that the differential expression of these two proteins reflected the difference in protein contents between normal and tumor cells in the sample tissues.

The results obtained using SDS-PAGE/Western blotting and immunohistochemistry lead us to the conclusion that spot 14991 included two proteins with different expression patterns. RKIP expression did not contribute to a higher intensity of spot 14991 in tumor tissues, probably because the absolute RKIP expression level was lower than that of MnSOD.

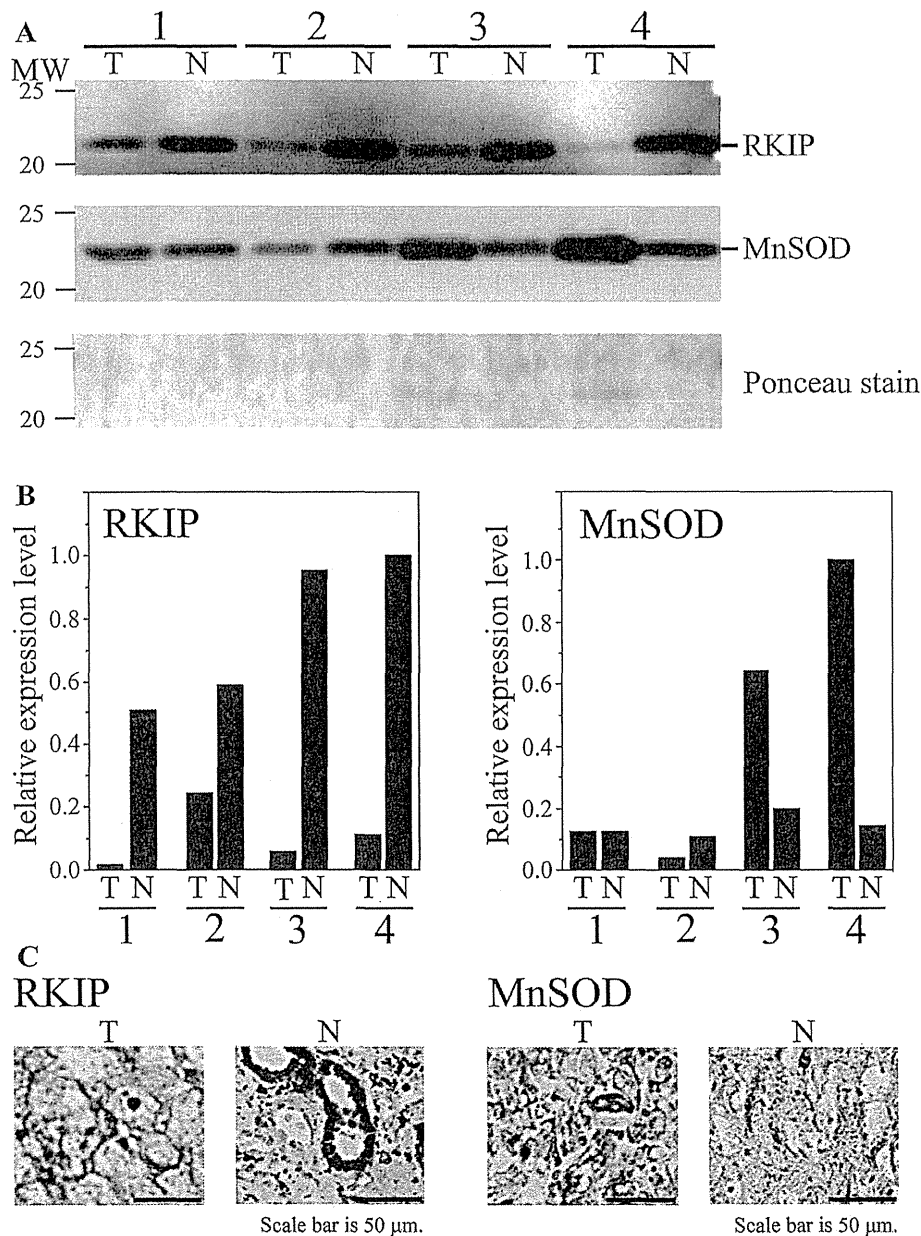


**Fig. 2** – Validation of the difference in spot 14991 intensity between tumor and non-tumor tissues using specific antibodies. **(A)** Expression of raf-1 kinase inhibitory protein (RKIP) and manganese superoxide dismutase (MnSOD) in the 9 ccRCC cases analyzed by Western blotting. The expected molecular mass of RKIP is 21,057 Da, and that of MnSOD was 20,696 Da. **(B)** The bar graph represents relative band intensities normalized to loading control. **(C)** Expression of RKIP and MnSOD by immunohistochemistry. Note that RKIP expression was observed in proximal tubular cells, while MnSOD was localized to tumor cells.

We speculated that MnSOD was predominantly represented in spot 14991, although RKIP had a higher MasCot score and number of peptides than MnSOD.

### 3.3. Clinical relevance of RKIP and MnSOD revealed by immunohistochemistry

To evaluate the clinical relevance of RKIP and MnSOD in ccRCC, we performed immunohistochemical analysis of the other 99 ccRCC cases.

A Kaplan–Meyer survival curve showed that the RKIP expression did not have prognostic value for progression-free and overall survival (Fig. 3A and B) and did not show significant association with any clinical and pathological parameters (Table 1). In contrast, Moon et al. [31], in their immunohistochemical study, showed that RCC patients with a lower RKIP expression had shorter survival. The discrepancy between those and our results may be attributed to differences in patient treatments after surgical tumor resection.

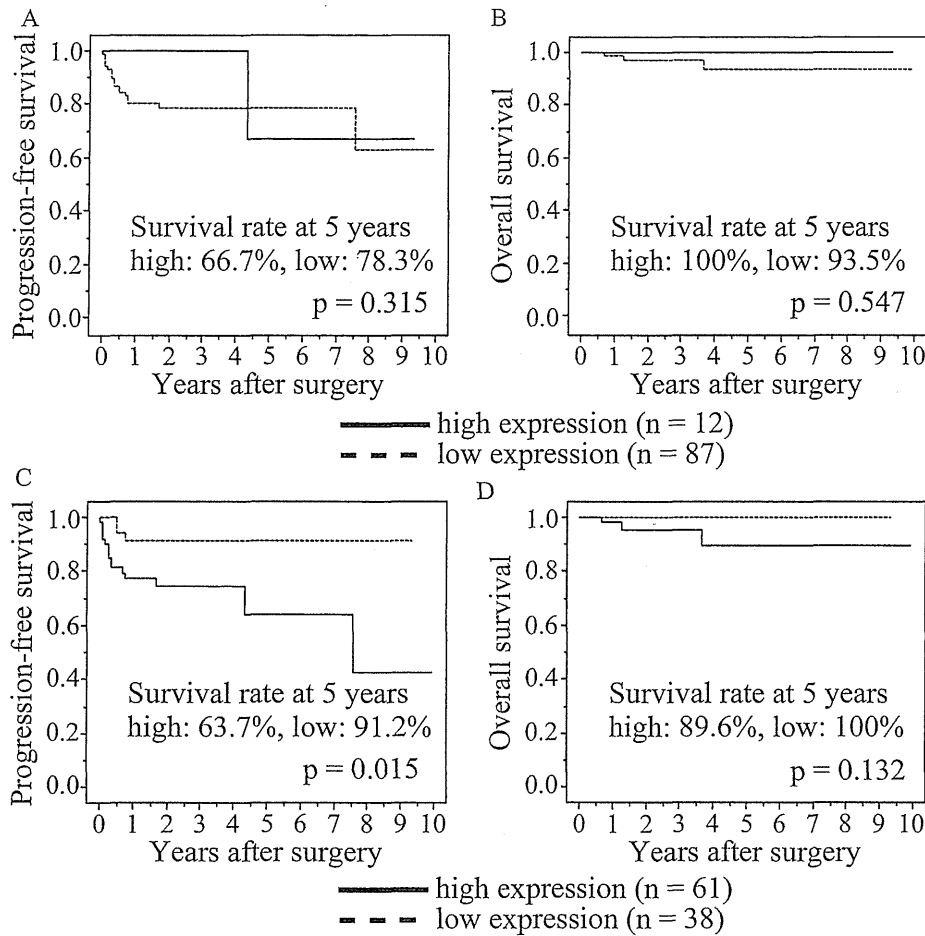


**Fig. 3 – RKIP and MnSOD expression and prognosis. RKIP expression did not significantly correlate with disease-free (A) or overall (B) survival. MnSOD expression showed significant correlation with disease-free (C), but not overall (D) survival.**

In the previous immunohistochemical report, adjuvant treatments were not mentioned [31], while the patients in our study received adjuvant therapy (Supplemental Table 1). This difference in treatments may affect the correlation between RKIP expression and post-surgical prognosis, and, in this case, RKIP expression may serve as a predictive biomarker for the adjuvant treatment of ccRCC patients. Moon et al. also found a significant association of RKIP expression with such clinical and pathological parameters as tumor size, stage, and metastasis [31], while our findings indicate that there is no correlation between RKIP expression and the examined clinicopathological parameters (Table 1). The differences in patients' cohorts and assessment of RKIP expression may account for this discordance. Multi-institutional immunohistochemical studies with uniform criteria may be required to address these issues.

The patients with a higher MnSOD expression level had poorer prognosis in terms of progression-free survival (Fig. 3C), but not overall survival (Fig. 3D). This is the first report about the prognostic value of the high MnSOD expression observed in ccRCC. Probably because the patients in this study received adjuvant treatments after tumor recurrence, overall survival did not vary significantly among patients with different levels

of MnSOD expression (Supplemental Table 1). A multivariate analysis of immunohistochemical data revealed that T stage, status of lymph node and distant metastasis, mode of infiltration, vascular invasion and MnSOD levels were significant indicators of progression-free survival, and only metastasis status was an independent prognostic factor (Table 2). These observations may suggest the association of MnSOD with the malignant potential of ccRCC cells, while further functional studies on the role of MnSOD cancer are required to validate these observations.

### 3.4. Functional significance of RKIP and MnSOD differential expression

Although a possible prognostic value of RKIP was suggested in a previous study, the effects of RKIP on RCC cells were not analyzed [31]. To examine the backgrounds of clinical significances of RKIP expression, we conducted an siRNA gene silencing assay for RKIP in ccRCC cells (Fig. 4). Transfection of ccRCC cells with RKIP-specific siRNA reduced the RKIP expression level (Fig. 4A, left panel), while cell growth and invasion significantly increased (Fig. 4B and C, left panels), indicating that RKIP may have tumor suppressive effects in ccRCC.

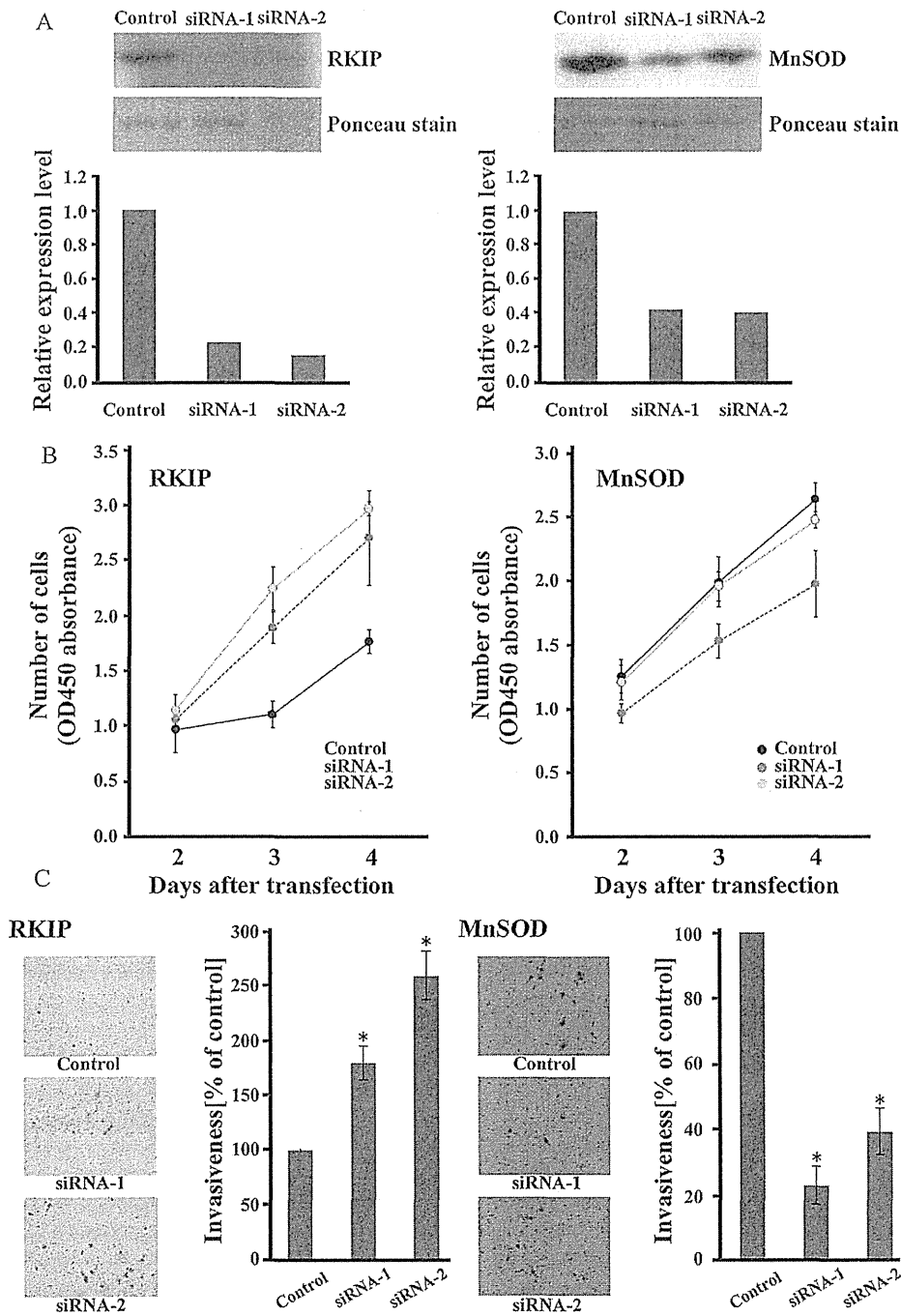


Fig. 4 – Effects of RKIP and MnSOD on tumor cell behavior in vitro. (A) In Caki-1 cells, RKIP and MnSOD expression was significantly inhibited by specific siRNAs. (B) RKIP silencing significantly promoted the proliferation of cells transfected with siRNA1 (days 3 and 4), and siRNA2 (day 4) (left panel). (C) Reduction in RKIP expression promoted (left panel), while reduction in MnSOD expression suppressed (right panel), tumor cell invasion.

A similar gene silencing assay for MnSOD in ccRCC cells showed that both siRNAs against MnSOD reduced MnSOD expression (Fig. 4A, right panel); however, cell proliferation was significantly affected only by siRNA1, and not by siRNA2 (Fig. 4B). These results suggest that the observed siRNA1 inhibition of cell proliferation may be due to off-target effects,

and MnSOD may not influence cell growth. On the other hand, tumor invasion was significantly inhibited by treatment with both MnSOD-specific siRNAs (Fig. 4C), suggesting that MnSOD may affect tumor cell invasion, but not cell proliferation. These observations are consistent with the association of MnSOD expression with shorter progression-free

**Table 2 – Univariate and multivariate analysis of progression-free survival.**

Features	Categories	Log-rank test	Cox proportional hazard model		
		<i>p</i> value	Hazard ratio	95% confidence interval	<i>p</i> value
Age	≤63	0.575			
	>63				
Gender	Male	0.471			
	Female				
T stage	1	0.0187	1.291	0.661–2.520	0.455
	2				
	3				
Lymph node	No	0.004	5.651	1.163–27.462	0.032
	Yes				
Metastasis	No	<0.001	7.872	2.616–23.684	< 0.001
	Yes				
Grade	1, 2	0.760			
	3, 4				
Mode of infiltration	a	0.017	1.019	0.335–3.097	0.974
	b, c				
Vascular invasion	No	0.002	0.974	0.229–3.337	0.944
	Yes				
MnSOD	Low	0.015	1.637	0.836–3.207	0.151
	High				

survival of ccRCC patients (Fig. 3C). Chen et al. [40] reported that MnSOD promoted tumor cell invasion, migration, and anchorage-independent soft-agar colony growth potentials through activation of FoxM1 and MMP2 in lung cancer cells, suggesting that the two malignancies, ccRCC and lung cancer, may share common molecular mechanisms of cell protection against reactive oxygen species.

#### 4. Conclusion

In proteomic studies using 2D-PAGE, the spot overlapping problem cannot be avoided even if samples are highly fractionated prior to separation by electrophoresis [7,8]. Although this problem has been emphasized in a previous report [6], only one protein per spot has usually been subjected to further analyses. In this report, we investigated two proteins identified in a single spot and revealed a novel association of these proteins, RKIP and MnSOD, with the malignant potential of ccRCC.

The detailed characterization of ccRCC molecular mechanisms is required to determine the optimal combination of tumor-suppressing agents [41]. Clinical outcome for the ccRCC patients varied even among patients of the same clinical stage, and specific molecular biomarkers are needed to complement the existing classification system [42]. Studies on the prognostic potential of RKIP and MnSOD may contribute to a better understanding of the molecular mechanisms underlying ccRCC progression and improve the clinical outcome for ccRCC patients. We consider that the proteins identified by tissue proteomics can be practically used as tissue biomarkers, not urine biomarkers. After surgical operation, surgical specimens are almost always available without additional invasive treatments, and tumor tissues may directly reflect the

characters of tumor cells. The clinical utilities of the identified proteins are also of interesting subjects.

Our study provides valuable technical insights into proteomic analysis by 2D-PAGE. Firstly, when multiple proteins are identified in a single protein spot, other methods, such as Western blotting, should be used to determine which of the proteins contribute to the intensity difference. In our study, the two identified proteins had opposite expression patterns, and Western blotting analysis clearly demonstrated that MnSOD contributed to higher spot intensity in tumor tissue samples. If the identified proteins show the same expression pattern, we need to separately evaluate their contributions to spot intensity. Secondly, several of the proteins identified in a single spot may be worth subjecting to further validation and functional studies. There are a number of cases when the 2D-PAGE results were not consistent with those obtained by SDS-PAGE/Western blotting, and such a discrepancy was attributed to variations in isoelectric points [43]. Our study indicates that expression of a protein with a higher Mascot score and peptide number may not always contribute to higher spot intensity. When validation of the most promising protein candidate by SDS-PAGE/Western blotting was not consistent with the 2D-PAGE data, the other identified proteins may need to be examined. Thirdly, it may be worth investigating the proteins with intensities that are not significantly different between experimental and control samples. Presently, there is no statistical data to estimate how frequently proteins overlap in a single protein spot, and it is possible that such spots may contain proteins with various expression patterns and important biological and clinical functions. This notion may lead to the idea of using 2D-PAGE as a pre-fractionation step. Thus, Thiede et al. [44] separated protein samples after stable isotope labeling with amino acids in cell culture (SILAC) using 2D-PAGE, then identified and compared proteins in

spots by LC-MS/MS. As 2D-PAGE demonstrates high separation performance, the complexity of the proteome can be reduced by 2D-PAGE fractionation prior to MS analysis. SILAC can only be used for tissue culture cells [44], while label-free MS expression profiling following 2D-PAGE separation may be applicable for clinical samples. This approach combines high-performance 2D-PAGE separation with high LC-MS/MS sensitivity, which should provide further insights into cancer proteomics and contribute to the translation of proteomic information into medical advances. Our proteomic study suggested the clinical utility of RKIP and MnSOD in the RCC patients. Especially, the clinical significances of RKIP should be further examined, because our findings that RKIP had tumor promoting effects were opposite to the previous report [31]. As RKIP is an endogenous inhibitor of signal transduction pathway [22], which is targeted by the molecular targeting drug such as sorafenib [21], the clinical application of RKIP is of intriguing in RCC.

### Conflict of interest

There are no conflicts of interest to disclose.

### Funding

This study was funded by the National Cancer Center Research Core Facility and Development Fund (23-A-7).

### Acknowledgement

We appreciate Dr. Hidenori Kanno (Department of Urology, Yamagata University Faculty of Medicine, Yamagata, Japan) for his kind help in the validation study on RKIP and MnSOD.


### REFERENCES

- [1] Weiss W, Gorg A. High-resolution two-dimensional electrophoresis. *Methods Mol Biol* 2009;564:13–32.
- [2] Gorg A, Obermaier C, Boguth G, Harder A, Scheibe B, Wildgruber R, et al. The current state of two-dimensional electrophoresis with immobilized pH gradients. *Electrophoresis* 2000;21:1037–53.
- [3] Weiss W, Weiland F, Gorg A. Protein detection and quantitation technologies for gel-based proteome analysis. *Methods Mol Biol* 2009;564:59–82.
- [4] Unlu M, Morgan ME, Minden JS. Difference gel electrophoresis: a single gel method for detecting changes in protein extracts. *Electrophoresis* 1997;18:2071–7.
- [5] Yamada M, Fujii K, Koyama K, Hirohashi S, Kondo T. The proteomic profile of pancreatic cancer cell lines corresponding to carcinogenesis and metastasis. *J Proteomics Bioinform* 2009;02:001–18.
- [6] Campostrini N, Areces LB, Rappsilber J, Pietrogrande MC, Dondi F, Pastorino F, et al. Spot overlapping in two-dimensional maps: a serious problem ignored for much too long. *Proteomics* 2005;5:2385–95.
- [7] Okano T, Kondo T, Kakisaka T, Fujii K, Yamada M, Kato H, et al. Plasma proteomics of lung cancer by a linkage of multi-dimensional liquid chromatography and two-dimensional difference gel electrophoresis. *Proteomics* 2006;6:3938–48.
- [8] Kosaihira S, Tsunehiro Y, Tsuta K, Tochigi N, Gemma A, Hirohashi S, et al. Proteome expression database of lung adenocarcinoma: a segment of the Genome Medicine Database of Japan Proteomics. *J Proteome Bioinform* 2009;2:463–5.
- [9] Hosoya N, Sakumoto M, Nakamura Y, Narisawa T, Bilim V, Motoyama T, et al. Proteomics identified nuclear N-myc downstream-regulated gene 1 as a prognostic tissue biomarker candidate in renal cell carcinoma. *Biochim Biophys Acta* 2013.
- [10] Rini BI, Campbell SC, Escudier B. Renal cell carcinoma. *Lancet* 2009;373:1119–32.
- [11] Sobin L, Gospodarowicz M, Wittekind C. 7th TNM Classification of Malignant Tumours. 7th ed. Wiley-Blackwell; 2009.
- [12] Fuhrman SA, Lasky LC, Limas C. Prognostic significance of morphologic parameters in renal cell carcinoma. *Am J Surg Pathol* 1982;6:655–63.
- [13] Kondo T, Hirohashi S. Application of highly sensitive fluorescent dyes (CyDye DIGE Fluor saturation dyes) to laser microdissection and two-dimensional difference gel electrophoresis (2D-DIGE) for cancer proteomics. *Nat Protoc* 2007;1:2940–56.
- [14] Moore MK, Viselli SM. Staining and quantification of proteins transferred to polyvinylidene fluoride membranes. *Anal Biochem* 2000;279:241–2.
- [15] Pearson K. On the criterion that a given system of deviations from the probable in the case of a correlated system of variables is such that it can be reasonably supposed to have arisen from random sampling. *Philos Mag* 1900;50:157–75.
- [16] Yates F. Contingency table involving small numbers and the  $\chi^2$  test. *J R Stat Soc* 1934;1:217–35.
- [17] Kaplan E, Meier P. Nonparametric estimation from incomplete observations. *J Am Stat Assoc* 1958;53:457–81.
- [18] Mantel N. Evaluation of survival data and two new rank order statistics arising in its consideration. *Cancer Chemother Rep* 1966;50:163–70.
- [19] Cox D. Regression models and life tables. *J R Stat Soc* 1972;34:187–220.
- [20] Student. On the error of counting with a haemocytometer. *Biometrika* 1907;5:351–60.
- [21] Escudier B, Eisen T, Stadler WM, Szczylik C, Oudard S, Siebels M, et al. Sorafenib in advanced clear-cell renal-cell carcinoma. *N Engl J Med* 2007;356:125–34.
- [22] Yeung K, Seitz T, Li S, Janosch P, McFerran B, Kaiser C, et al. Suppression of Raf-1 kinase activity and MAP kinase signalling by RKIP. *Nature* 1999;401:173–7.
- [23] Chatterjee D, Sabo E, Tavares R, Resnick MB. Inverse association between Raf Kinase Inhibitory Protein and signal transducers and activators of transcription 3 expression in gastric adenocarcinoma patients: implications for clinical outcome. *Clin Cancer Res* 2008;14:2994–3001.
- [24] Al-Mulla F, Hagan S, Behbehani AI, Bitar MS, George SS, Going JJ, et al. Raf kinase inhibitor protein expression in a survival analysis of colorectal cancer patients. *J Clin Oncol* 2006;24:5672–9.
- [25] Hagan S, Al-Mulla F, Mallon E, Oien K, Ferrier R, Gusterson B, et al. Reduction of Raf-1 kinase inhibitor protein expression correlates with breast cancer metastasis. *Clin Cancer Res* 2005;11:7392–7.
- [26] Li HZ, Wang Y, Gao Y, Shao J, Zhao XL, Deng WM, et al. Effects of raf kinase inhibitor protein expression on metastasis and progression of human epithelial ovarian cancer. *Mol Cancer Res* 2008;6:917–28.
- [27] Schuierer MM, Bataille F, Weiss TS, Hellerbrand C, Bosserhoff AK. Raf kinase inhibitor protein is downregulated in hepatocellular carcinoma. *Oncol Rep* 2006;16:451–6.

- [28] Kim HS, Kim GY, Lim SJ, Park YK, Kim YW. Reduced expression of Raf-1 kinase inhibitory protein is a significant prognostic marker in patients with gallbladder carcinoma. *Hum Pathol* 2010;41:1609-16.
- [29] Kim HS, Kim GY, Lim SJ, Kim YW. Loss of Raf-1 kinase inhibitory protein in pancreatic ductal adenocarcinoma. *Pathology* 2010;42:655-60.
- [30] Martinho O, Gouveia A, Silva P, Pimenta A, Reis RM, Lopes JM. Loss of RKIP expression is associated with poor survival in GISTs. *Virchows Arch* 2009;455:277-84.
- [31] Moon A, Park JY, Sung JY, Park YK, Kim YW. Reduced expression of Raf-1 kinase inhibitory protein in renal cell carcinoma: a significant prognostic marker. *Pathology* 2012;44:534-9.
- [32] Fridovich I. Superoxide radical and superoxide dismutases. *Annu Rev Biochem* 1995;64:97-112.
- [33] Zhang Y, Gu J, Zhao L, He L, Qian W, Wang J, et al. Complete elimination of colorectal tumor xenograft by combined manganese superoxide dismutase with tumor necrosis factor-related apoptosis-inducing ligand gene virotherapy. *Cancer Res* 2006;66:4291-8.
- [34] Li S, Yan T, Yang JQ, Oberley TD, Oberley LW. The role of cellular glutathione peroxidase redox regulation in the suppression of tumor cell growth by manganese superoxide dismutase. *Cancer Res* 2000;60:3927-39.
- [35] Mohr A, Buneker C, Gough RP, Zwacka RM. MnSOD protects colorectal cancer cells from TRAIL-induced apoptosis by inhibition of Smac/DIABLO release. *Oncogene* 2008;27:763-74.
- [36] Zhang HJ, Zhao W, Venkataraman S, Robbins ME, Buettner GR, Kregel KC, et al. Activation of matrix metalloproteinase-2 by overexpression of manganese superoxide dismutase in human breast cancer MCF-7 cells involves reactive oxygen species. *J Biol Chem* 2002;277:20919-26.
- [37] Durak I, Beduk Y, Kavutcu M, Ozturk S, Canbolat O, Ulutepe S. Activities of superoxide dismutase and glutathione peroxidase enzymes in cancerous and non-cancerous human kidney tissues. *Int Urol Nephrol* 1997;29:5-11.
- [38] Melov S, Coskun P, Patel M, Tuinstra R, Cottrell B, Jun AS, et al. Mitochondrial disease in superoxide dismutase 2 mutant mice. *Proc Natl Acad Sci U S A* 1999;96:846-51.
- [39] Trachootham D, Alexandre J, Huang P. Targeting cancer cells by ROS-mediated mechanisms: a radical therapeutic approach. *Nat Rev Drug Discov* 2009;8:579-91.
- [40] Chen PM, Wu TC, Shieh SH, Wu YH, Li MC, Sheu GT, et al. MnSOD promotes tumor invasion via upregulation of FoxM1-MMP2 axis and related with poor survival and relapse in lung adenocarcinomas. *Mol Cancer Res* 2013;11:261-71.
- [41] Singer EA, Gupta GN, Marchalik D, Srinivasan R. Evolving therapeutic targets in renal cell carcinoma. *Curr Opin Oncol* 2013;25:273-80.
- [42] Brookman-May S, May M, Shariat SF, Xylinas E, Stief C, Zigeuner R, et al. Features associated with recurrence beyond 5 years after nephrectomy and nephron-sparing surgery for renal cell carcinoma: development and internal validation of a risk model (PRELANE score) to predict late recurrence based on a large multicenter database (CORONA/SATURN project). *Eur Urol* 2013;64:472-7.
- [43] Muto T, Taniguchi H, Kushima R, Tsuda H, Yonemori H, Chen C, et al. Global expression study in colorectal cancer on proteins with alkaline isoelectric point by two-dimensional difference gel electrophoresis. *J Proteomics* 2011;74:858-73.
- [44] Thiede B, Koehler CJ, Strozynski M, Treumann A, Stein R, Zimny-Arndt U, et al. High resolution quantitative proteomics of HeLa cells protein species using stable isotope labeling with amino acids in cell culture (SILAC), two-dimensional gel electrophoresis (2DE) and nano-liquid chromatography coupled to an LTQ-OrbitrapMass spectrometer. *Mol Cell Proteomics* 2013;12:529-38.

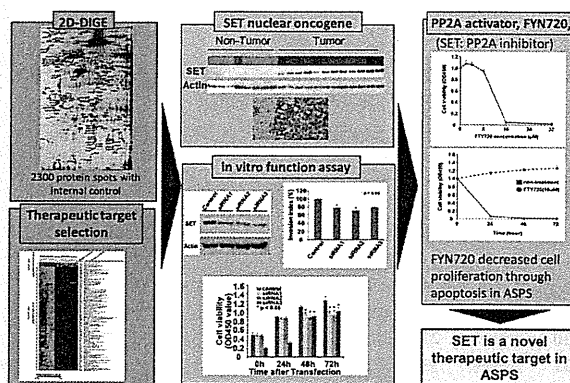


# Proteomics Identified Overexpression of SET Oncogene Product and Possible Therapeutic Utility of Protein Phosphatase 2A in Alveolar Soft Part Sarcoma

Daisuke Kubota,<sup>†,‡</sup> Akihiko Yoshida,<sup>§</sup> Akira Kawai,<sup>‡</sup> and Tadashi Kondo<sup>\*,†</sup><sup>†</sup>Division of Pharmacoproteomics, National Cancer Center Research Institute, Tsukiji 5-1-1, Chuo-ku, Tokyo 104-0045, Japan<sup>‡</sup>Division of Musculoskeletal Oncology and <sup>§</sup>Pathology and Clinical Laboratory Division, National Cancer Center Hospital, Tsukiji 5-1-1, Chuo-ku, Tokyo 104-0045, Japan Supporting Information

**ABSTRACT:** Alveolar soft part sarcoma (ASPS) is an exceedingly rare sarcoma refractory to standard chemotherapy. Although several molecular targeting drugs have been applied for ASPS, their clinical significance has not yet been established, and novel therapeutic strategies have long been required. The aim of this study was to identify proteins aberrantly regulated in ASPS and to clarify their clinical significance. Protein expression profiling of tumor and nontumor tissues from 12 ASPS patients was performed by 2-D difference gel electrophoresis and mass spectrometry. We found that the expression of 145 proteins differed significantly. Among them, further investigation was focused on the SET protein, which has multifunctional roles in cancers. Immunohistochemistry confirmed overexpression of SET in all 15 ASPS cases examined. Gene silencing of SET significantly decreased cell proliferation, invasion, and migration against a background of induced apoptosis. SET is known to be an inhibitor of phosphatase 2A (PP2A), which functions as a tumor suppressor by inhibiting the signal transduction pathway and inducing apoptosis. We found that a PP2A activator, FYN720, decreased cell proliferation through apoptosis. Together, our findings may suggest the possible contribution of SET to the tumor progression and the utility of FYN720 for treatment of ASPS.

## Proteomic approach to novel therapeutic target in Alveolar Soft Part Sarcoma



## 1. INTRODUCTION

Alveolar soft part sarcoma (ASPS) is an exceedingly rare sarcoma that accounts for fewer than 1% of all soft tissue sarcomas.<sup>1</sup> While patients can often achieve prolonged survival after surgery, even if metastases are present, most eventually succumb to the disease as a result of late metastasis. Both standard cytotoxic chemotherapy and radiation therapy have no significant survival advantage, and an effective molecular targeting drug has long been sought. ASPS is characterized by the presence of chromosomal rearrangement at 17q25 and Xp11.2, engendering a fusion gene, ASPSCR1-TFE3, which is a superactivated chimeric transcription factor.<sup>2</sup> Recent global gene expression profiling has identified an array of genes that are possibly regulated by the ASPSCR1-TFE3 fusion gene, and these genes include potentially therapeutic targets.<sup>3–3</sup> One of the critical genes induced by ASPSCR1-TFE3 and playing a role in disease progression is the angiogenesis-promoting oncogene, MET.<sup>3</sup> This molecular background has led to the introduction of antiangiogenic agents such as INF- $\alpha$ ,<sup>6–8</sup> bevacizumab,<sup>9,10</sup> sunitinib,<sup>11–13</sup> and cediranib for ASPS. The clinical efficacies of

these novel molecular targeting agents will be validated in large-scale clinical studies.

In the present investigation, in order to clarify the molecular pathogenesis of ASPS and identify proteins that might have clinical utility, we performed a proteomic study of ASPS. While proteomics has been applied to a variety of cancers to identify biomarkers and therapeutic targets,<sup>14</sup> no proteomics study of ASPS has been reported, except for one in which only one formalin-fixed and paraffin-embedded ASPS tissue was examined using a shotgun approach.<sup>15</sup> We identified proteins that were uniquely expressed in the tumor tissues, and further focused on one oncogene product, suppressor of variegation, enhancer of zeste, and trithorax (SET), which was originally reported as a chimeric gene in acute myelocytic leukemia.<sup>16</sup> We confirmed the overexpression of SET in ASPS by Western blotting and immunohistochemistry and verified the functional significance of SET by a gene-silencing assay. SET is a specific inhibitor of a

Received: September 12, 2013

tumor suppressor, phosphatase 2A (PP2A),<sup>17</sup> which is deregulated in several malignancies.<sup>18</sup> We revealed that a PP2A activator, FYN720, exerted antitumor effects on ASPS cells. Our study reveals novel aspects of SET in ASPS and suggests possible therapeutic application of a PP2A inhibitor for this malignancy.

## 2. MATERIALS AND METHODS

### 2.1. Patients, Cell Line, and Protein Samples

This study included all 15 cases of ASPS that had been diagnosed and treated at the National Cancer Center Hospital between 1996 and 2010. Metastasis was diagnosed by computed tomography. For proteomics, tumor samples were obtained from 12 cases at the time of surgery, snap frozen in liquid nitrogen, and stored until use. The adjacent nontumor tissues were also obtained from areas distant from the tumor margin in 8 of these 12 cases. Immunohistochemistry was performed for all 15 ASPS cases including the 12 cases used for proteomics. Clinical information on the 15 patients is detailed in Table 1. Protein

**Table 1. Summary of Clinicopathological Data of the 15 ASPS Patients**

no.	gender	age	location	metastasis
ASPS-1	female	28	femur	none
ASPS-2	female	26	retroperitoneal	recurrence, spleen, bone
ASPS-3	female	23	pelvis	neck, brain
ASPS-4	female	23	buttock	lung
ASPS-5	female	16	femur	lung
ASPS-6	male	35	extremity	bone, lung, brain
ASPS-7	female	29	buttock	lung
ASPS-8	female	14	extremity	none
ASPS-9	male	33	extremity	lung
ASPS-10	female	27	pelvis	lung
ASPS-11	female	33	pelvis	lung
ASPS-12	male	31	femur	lung
ASPS-13	female	47	primary unknown	brain
ASPS-14	female	26	extremity	brain, lung
ASPS-15	female	23	extremity	brain, lung

contents of the primary tumor tissues were examined in three cases each of gastrointestinal stromal tumor, osteosarcoma, rhabdomyosarcoma, and epithelioid sarcoma (Supplementary Table 1 in the Supporting Information). Protein extracts from normal tissues were obtained from BioChain (Newark, CA). The ASPS cell line ASPS-KY was kindly provided by Dr. Y Miyagi (Kanagawa Cancer Center Research Institute, Kanagawa, Japan). ASPS-KY was cultured in DMEM (supplemented with 10% fetal bovine serum, 1 mmol/L sodium pyruvate, 1 × nonessential amino acids, and 2 mmol/L glutamine) and incubated at 37 °C in a humidified 5% CO<sub>2</sub> atmosphere. This project was approved by the ethical review board of the National Cancer Center, and signed informed consent was obtained from all of the patients included.

### 2.2. Protein Expression Profiling

Proteins were extracted from frozen tissues in accordance with our previous report.<sup>19</sup> In brief, frozen tissues were crushed to powder with a Multibeads shocker (Yasui Kikai, Osaka, Japan) in liquid nitrogen. The frozen powder was then treated with urea lysis buffer (6 M urea, 2 M thiourea, 3% CHAPS, 1% Triton X-100) and centrifuged at 15 000 rpm for 30 min. The supernatant was recovered and stored at -80 °C until use.

Protein expression profiling was performed by 2D-DIGE with our original large-format electrophoresis apparatus.<sup>19</sup>

The experiment design for the 2D-DIGE experiments is overviewed in Figure 1A. In brief, the internal standard sample was created by mixing equal portions of all individual samples. Five micrograms each of the internal standard sample and individual sample were labeled with Cy3 and Cy5, respectively (CyDye DIGE Fluor saturation dye, GE, Uppsala, Sweden). These differently labeled protein samples were mixed and separated according to isoelectric point and molecular weight. The first-dimension separation was achieved using Immobiline pH gradient DryStrip gels (24 cm long, pI range 4–7, GE) and Multiphor II (GE). The second-dimension separation was achieved by SDS-PAGE using our original large-format electrophoresis apparatus (33 cm separation distance, Biocraft, Tokyo, Japan).<sup>19</sup> The gels were scanned using laser scanners (Typhoon Trio, GE) at appropriate wavelengths for Cy3 or Cy5 (Figure 1B). For all protein spots, the Cy5 intensity was normalized with the Cy3 intensity in the same gel using the ProgenesisSameSpots software package version 3 (Nonlinear Dynamics, Newcastle-upon-Tyne, U.K.). All samples were examined in triplicate gels, and the mean normalized intensity value was calculated. The experimental reproducibility of 2D-DIGE was examined by running the identical sample three times and evaluating the correlation of the protein spot intensities on a scatter gram (Figure 1C). Mass spectrometric protein identification was performed according to our previous report.<sup>19</sup> In brief, 100 μg of the protein sample was labeled with Cy5 and separated by 2D-PAGE as previously mentioned. Protein spots were recovered from the gels by an automated spot recovery machine (Molecular Hunter, AsOne, Osaka, Japan) and subjected to manual in-gel digestion using trypsin.<sup>19</sup> The tryptic digests were subjected to liquid chromatography coupled with nanoelectrospray tandem mass spectrometry (Finnigan LTQ Orbitrap XL mass spectrometer, Thermo Electron, San Jose, CA). The Mascot software package (version 2.2; Matrix Science, London, U.K.) was used to search for the mass of each peptide ion peak against the SWISS-PROT database (*Homo sapiens*, 471 472 sequences in the Sprot-57.5.fasta file). Proteins with a Mascot score of 34 or more were considered to be positively identified.

### 2.3. Western Blotting

Five microgram portions of the protein samples were separated by SDS-PAGE (ATTO, Tokyo, Japan). The separated proteins were subsequently blotted on a nitrocellulose membrane and incubated with a monoclonal antibody against SET (1:1000 dilution, Abcam, Cambridge, MA), pAKT(1:500 dilution, BD Bioscience, Franklin Lakes, NJ), Bad (1:500 dilution, BD), Bid (1:500 dilution, BD), and actin (1:5000, Abcam). The membrane was then reacted with horseradish-peroxidase-conjugated secondary antibody (1:3000 dilution, GE), processed using enhanced chemiluminescence reagents (ECL Prime, GE), and scanned with a LAS-3000 laser scanner (FujiFilm, Tokyo, Japan).

### 2.4. Immunohistochemistry

The most representative areas of tumor and nontumor tissues were sampled for tissue microarray (TMA). The TMAs were assembled with a tissue array instrument (Azumaya, Tokyo, Japan). To reduce sampling bias due to tumor heterogeneity, we used two replicate 2.0-mm-diameter cores from different areas of individual tumors. The TMA consisted of 15 cases of ASPS, including samples from the 12 cases (ASPS1–12) subjected to 2D-DIGE and from 3 newly enrolled cases (ASPS13–15, Table 1).

The expression levels of SET were examined immunohistochemically. In brief, 4-μm-thick formalin-fixed, paraffin-embedded tissue sections and TMAs were autoclaved in 10 mmol/L

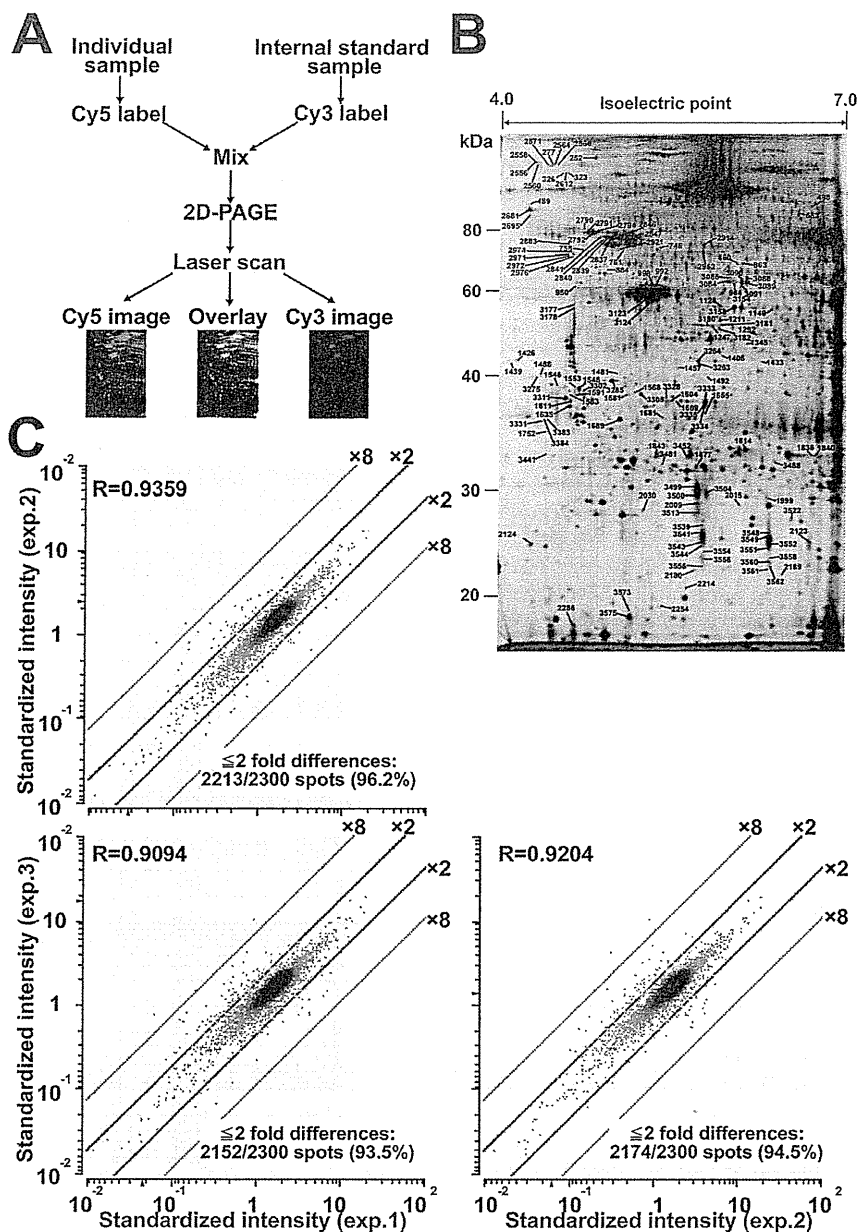


**Figure 1.** Overview of experiment workflow using 2D-DIGE. (A) Individual samples and internal standard sample were labeled with two different fluorescent dyes, mixed together, and separated by 2D-PAGE. (B) Typical gel image of 2D-DIGE. The protein spot numbers correspond to those in Figure 2, Table 2, and Supplementary Tables 2 and 3 in the Supporting Information. The enlarged image is provided in Supplementary Figure 1 in the Supporting Information. (C) Technical reproducibility was examined by running one identical sample three times. Note that the intensity of at least 93.5% of the protein spots was scattered within a two-fold difference, and the overall correlation coefficient was more than 0.9.

citrate buffer (pH 6.0) at 121 °C for 30 min and incubated with anti-SET antibody (1:500 dilution, Abcam) for 1 h. Immunostaining was carried out by the streptavidin–biotin peroxidase method using an ABC complex/horseradish peroxidase kit (DAKO, Glostrup, Denmark). One pathologist (A.Y.) and one clinician (D.K.) reviewed the stained sections.

## 2.5. Gene Silencing Assay

SET-specific siRNAs were purchased from Sigma-Aldrich, and control stealth siRNA was from Life Technologies. The target sequences were 5'-rGrCrAUUUrAUUUrGrArCrCrArGrArGUUTT-3'

(siRNA-1), 5'-rCrArGrArGUUrGrArArGUrGrArCrArGrArATT-3' (siRNA-2), and 5'-rGrCrAUUUrAUUUrGrArCrCrArGrArGUUTT-3' (siRNA-3). A total of  $5 \times 10^3$  ASPs cells, ASPS-KY, were seeded into each well of a 96-well plate (Coaster, Cambridge, MA). The following day, the cell monolayer was washed with prewarmed sterile phosphate-buffered saline. Cells were transfected with the appropriate siRNA using DharmaFECT transfection reagents (Thermo Fisher, Waltham, MA) in accordance with the manufacturer's protocol. Twenty-four hours later the culture medium for the transfected cells was switched to medium A, whereas the conditioned medium was not changed.

2.6. Cell Proliferation and Invasion Assay

To examine the effects of SET and an inhibitor for PP2A on the ASPS cells, cell proliferation was examined after treatment with siRNAs or a PP2A activator, FTY720 (Selleck Chemicals, Houston, TX). FTY720 was dissolved with dimethyl sulfoxide (DMSO, Wako, Osaka, Japan), and added to the culture medium at an appropriate concentration. Cell proliferation was examined by the tetrazolium-based colorimetric MTT assay. In brief, the cells were transfected with the appropriate siRNA using DharmaFECT transfection reagent for 24 h. Alternatively, the cells were incubated with various concentrations of FTY720. Then, 20 μL of the reagent from Cell Counting Kit-8 (Dojindo, Kumamoto, Japan) was added to each well containing ASPS-KY cells. After 2 h of incubation, the optical density was measured at a wavelength of 450 nm using a microplate reader (SAFARI, TECAN, Männedorf, Switzerland). Cell invasion before and after the treatments was evaluated using the BD BioCoat Invasion Chamber (BD Bioscience) in accordance with the manufacturer's protocol. In brief, the cells were transfected with the appropriate siRNA using DharmaFECT transfection reagent for 24 h. The cells were seeded onto the membrane in the upper chamber of the trans-well at a concentration of  $5 \times 10^5$  in 500 μL of serum-free medium. The medium in the lower chamber contained 10% fetal calf serum as a source of chemoattractants. Cells that passed through the Matrigel-coated membrane were stained with Diff-Quick (Sysmex, Kobe, Japan), and the cells were counted.

All experiments were performed at least three times, in duplicate or triplicate, and statistical significance was calculated by *t* test using the SPSS statistical software package (IBM, Armonk, NY).

3. RESULTS

3.1. Protein Expression Profiling Identifies the Set Oncogene Product in ASPS

Protein expression profiles were created by 2D-DIGE, which is advantageous in that gel-to-gel variations can be compensated for by normalizing the expression data for individual samples with those of the common internal standard sample using two different fluorescent dyes (Figure 1A). Such normalization was performed for 2300 protein spots (Figure 1B, the enlarged image is Supplementary Figure 1 in the Supporting Information, and the intensity of all 2300 protein spots is shown in Supplementary Table 2 in the Supporting Information). The large-format electrophoresis apparatus and the internal standard sample resulted in highly reproducible protein expression profiling, as shown by scatter gram for three independent experiments on one identical sample (Figure 1C).

The comparison between tumor and nontumor tissues resulted in the identification of 145 protein spots showing significant differences in intensity (*p* value less than 0.01 and more than two-fold intensity difference, Figure 2 and Table 2). Mass spectrometry detected the corresponding proteins for these 145 spots. The differential intensities of the protein spots and the results of protein identification are summarized in Figure 2. Detailed data for the identified proteins and supportive data for positive protein identification are provided in Supplementary Table 3 in the Supporting Information.

3.2. Immunological Validation of SET Overexpression in Primary Tumor Tissues of ASPS

We focused in detail on the higher expression of the SET oncogene product. The product of the SET is a multifunctional protein contributing to progression of various cancers and is

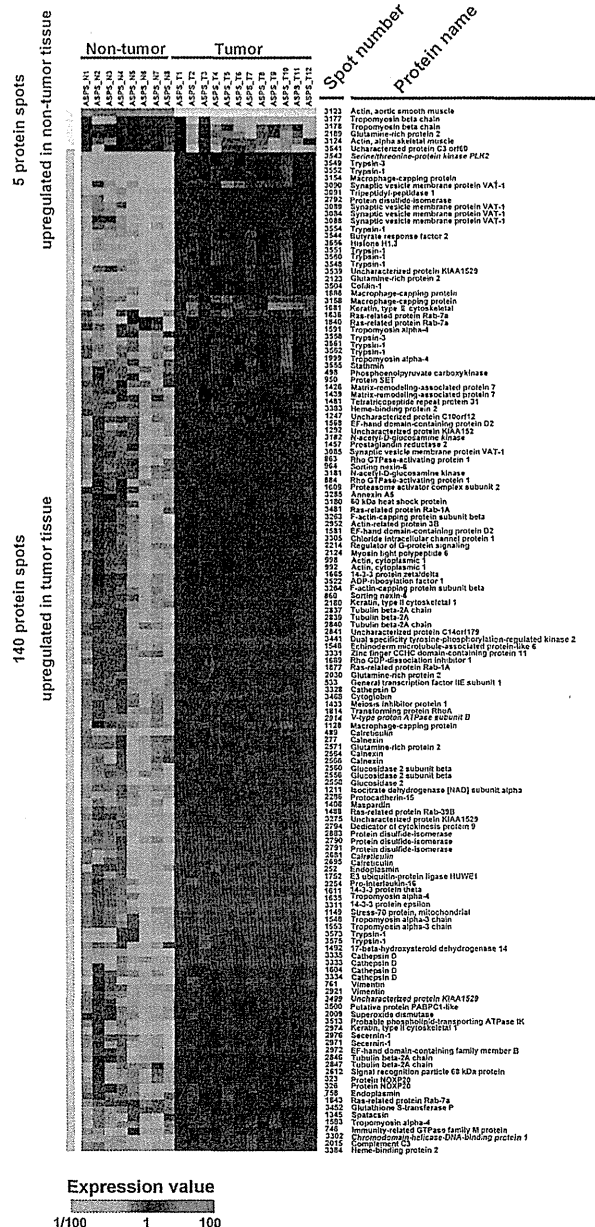


Figure 2. Protein spots with different intensities and their annotation by mass spectrometry. Differences in the intensity of protein spots between tumor tissues and noncancerous adjacent tissues are exhibited in the form of a heat-map. Any intensity showing more than a two-fold difference with statistical significance (*p* < 0.05) was considered to be positive. Mass spectrometry annotation of the protein spots is demonstrated on the right side of the heat-map.

considered to be a therapeutic target.<sup>20</sup> By Western blotting, we confirmed the overexpression of SET in tumor tissues compared with noncancerous adjacent normal tissues (Figure 3A). SET was observed as a single band with the expected molecular weight (Figure 3A). Immunohistochemistry demonstrated nuclear localization of SET with preferential expression in tumor cells relative to nontumor cells (Figure 3B). We confirmed the overexpression of SET in the 15 cases of ASPS (Supplementary